JOURNAL OF
PHYSICS AND CHEMISTRY
OF SOLIDS

ELSEVIER

Journal of Physics and Chemistry of Solids 62 (2001) 865–871

www.elsevier.nl/locate/jpcs

Influence of a small inhomogeneous broadening of Cr^{3+}:$LiSrAlF_6$ emission line on the laser performance

Viktor A. Fromzel*, Coorg R. Prasad

Science and Engineering Services, Inc., 4032 Blackburn Lane, Burtonsville, MD 20866, USA

Received 12 May 2000; accepted 2 August 2000

Abstract

Experimental investigations of Cr:LiSAF laser output spectra have shown that its emission line is inhomogeneously broadened. This is clearly evident from the fact that the measured laser line width is always much broader than what is possible due to 'spatial hole burning' in a Cr:LiSAF standing-wave resonator, if the Cr:LiSAF emission line is assumed to be homogeneously broadened. By assuming the possibility of a slight inhomogeneous broadening of the Cr:LiSAF emission line, corresponding to the $^4T_2$-$^4A_2$ transition of Cr^{3+}-ions, the observed laser line width can be explained. We have calculated the extent of laser output reduction due to inhomogeneous broadening, by means of a simple model. By comparing the measured laser output energy with the calculated laser output, the relative spectral inhomogeneity parameter β is estimated to be $\beta = 1.6$–1.8.

Keywords: A. Optical materials; B. Infrared spectroscopy; D. Optical properties

1. Introduction

In recent years, diode-pumped Cr^{3+}:$LiSrAlF_6$ (LiSAF) lasers have been successfully developed as an all-solid-state laser which can be used to replace the well-known Ti-sapphire laser in many applications [1,2]. The most attractive features of Cr:LiSAF lasers are their capability of being effectively directly pumped by AlGaInP laser diodes near 680 nm due to the relatively long excited-state radiative lifetime (67 μs), and a broad tunability, at least from 800 to 1000 nm, combined with the possibility of having a narrow laser line width [1–3]. These important features make Cr:LiSAF lasers an ideal source for high-resolution spectroscopy and airborne DIAL systems [4,5]. The broad emission of Cr:LiSAF, centered at ~840 nm, provides the capability of reaching the 820 and 940 nm H_2O absorption bands for making atmospheric water vapor measurements. A high output energy (~50 mJ/pulse) and a narrow line width (<300 MHz) of the laser are required for accurate DIAL measurements. Such a high energy diode-pumped laser is currently being built at SESI for use in an airborne water vapor DIAL system.

The ability to extract the maximum value of the stored energy from an excited laser medium in a single longitudinal mode, or in a narrow laser output line width, is determined by the nature of spectral broadening of the active medium emission line. It can be shown [6], that the extraction efficiency of a laser with a homogeneously broadened emission line is the same both in the case of a broad laser output line width and in single longitudinal mode operation. On the other hand, laser extraction efficiency can be quite different for these two regimes if the laser emission line has an evident inhomogeneous spectral broadening. Neodymium glass lasers are a good example of such of behavior.

So far, it has been assumed that Cr^{3+}-ions in $LiSrAlF_6$ crystal have a homogeneously broadened emission line for the $^4T_2$-$^4A_2$ transition because they replace only one type of nearly identically located Al-ions in the lattice [7,8]. As a result, an absence of any reduction in Cr:LiSAF laser efficiency is assumed both for broad line width operation and for a single longitudinal mode regime. But, as will be shown in this paper, certain features of Cr:LiSAF laser behavior clearly indicate the possibility that the laser emission line of the Cr^{3+}-ions in $LiSrAlF_6$ crystal is slightly inhomogeneously broadened. The broadening has influence both on

* Corresponding author. Tel.: +1-301-989-1896; fax: +1-301-421-4137.

E-mail address: vfromzel@sesi-md.com (V.A. Fromzel).

0022-3697/01/$ - see front matter
PII: S0022-3697(00)00241-9

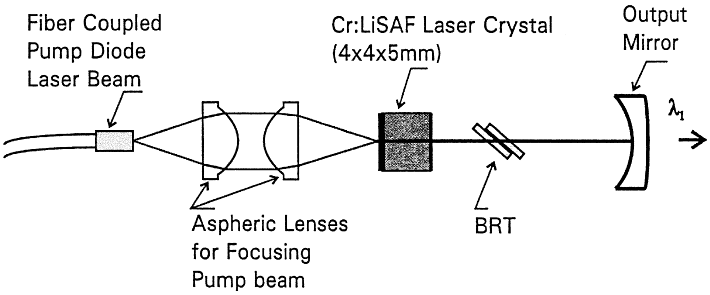

Fig. 1. Cr:LiSAF end-pumped laser schematic. The pump power from fiber coupled diode array is focused on the Cr:LiSAF crystal through the dichroic mirror by two aspheric lenses. The output coupler is a curved mirror (RoC = 20 cm, at 870–960 nm $R_{out} = 99.6–99.0\%$). BRT is the two-plate birefringent tuner.

the laser output spectrum, and on the laser efficiency when the laser is operated with a narrow line width. The spectroscopy features of Cr:LiSAF crystals [7] are not investigated enough to eliminate totally possibility of inhomogeneous broadening of these crystals. Laser operation with Cr:LiSAF crystals provides a very sensitive method of investigating the laser emission line broadening, because laser line width and energy extracted from the laser medium are both a function of spectral inhomogeneity of the laser emission line. In this paper, we present the results of an experimental investigation of Cr:LiSAF laser output linewidths for different pump levels. In these experiments, the laser energy output and spectral linewidths were measured in free running pulsed mode with narrow (0.03 nm) and very wide (13–20 nm) output line width for a wide range of pump values exceeding the laser threshold. Also presented is a comparison of experimental data with the theoretically expected laser line width for a homogeneously broadened emission line. The value of inhomogeneous broadening has been estimated by comparing the experimental and theoretically expected values of the laser output energy in free running operation for various values of inhomogeneous broadening of the emission line.

2. Experimental layout

An experimental study was performed with two types of diode-pumped Cr:LiSAF lasers in free running operation. The first laser was running in the μJ range of output energy. It utilized a 3% doped Cr:LiSAF crystal (3 × 3 × 5 mm, Lightning Optical Corporation) that was end-pumped by a cw 3W fiber coupled diode array (SDL-8300, Spectra Diode Laboratories) at a wavelength of 670 nm (Fig. 1) [9]. The pump power was focused on the flat end of the crystal to a spot size of 250 μm by two aspheric lenses ($f_1 = 6.24$ mm and $f_2 = 4.51$ mm).The pumped end of the crystal had a dichroic coating with a high transmission ($T > 93\%$) at 670 nm and a high reflection ® > 99.9%) in wavelength range of 870–960 nm. The other crystal end had an AR coating with a residual reflection of less than 0.2%for the wavelength range of 860–950 nm. The laser cavity consisted of a flat mirror on the Cr:LiSAF crystal end surface, and a concave output coupler with a radius of curvature $r_c = 20$ cm and reflection of $R_{out} = 99.6–99.0\%$ for the wavelength range of 870–960 nm. The cavity length was $L = 18$ cm and a TEM_{00} transverse mode operation was obtained. The laser beam is measured to be a diffraction limited beam ($M^2 \sim 1$) for all power levels. The TEM_{00} transverse mode diameter on the flat HR mirror (end of the crystal) was 220 μm. Pump pulse duration was about ~200 ms, pulse repetition rate was 100 Hz. Wavelength selection and tuning of the laser output spectrum was performed by an intra-cavity birefringent tuner (BRT) consisting of two or three crystalline quartz plates with thicknesses of 0.5 and 5.0 mm, or 0.5, 1.0 and 5.0 mm, respectively. The plates were mounted with their optical axes parallel to each other and were oriented at the Brewster angle in the cavity. The output beam of the Cr:LiSAF laser was linearly polarized (*E//c*) due to anisotropic spectroscopic features of Cr:LiSAF crystals. If the BRT was rotated about the perpendicular to the optical axis, approximately parallel to the polarization plane of the laser ($\omega = 0$), there was no laser output spectrum selection introduced by the BRT, except, of course, restriction of the output spectrum by the wavelength characteristics of the cavity mirror coatings. By rotating the BRT about the perpendicular so that the optical axis was positioned at some angle with the laser polarization plane, the laser output line width of 0.03 nm, centered at the same wavelength as the middle of the broad laser output spectrum located, could be achieved. By using this method of getting broad or very narrow laser line width, we can be sure that the difference in the laser performance is caused by only the difference in laser line width, not by other reasons (cavity losses, wavelength position, and ets.) which stay intact.

The second Cr:LiSAF laser that was used for these experiments was a high energy diode-pumped laser based on the double Total Internal Reflection (TIR) cavity shown in Fig. 2 [10] The 5.5% doped Cr:LiSAF slab (6 × 6 mm, 25 mm long) was pumped on two sides by eight 690 nm diode laser stacks (developed at Lawrence Livermore

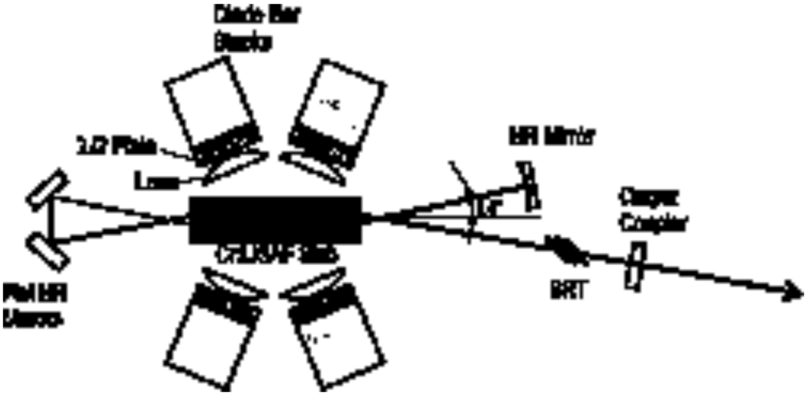

Fig. 2. Cr:LiSAF TIR cavity laser layout. Resonator consists of four mirrors: HR curved mirror (RoC = 200 cm, at 810–840 nm, $R_{out} = 99.5\%$), two HR flat mirrors (at 810–840 nm, 45°, $R_{out} = 99.5\%$), and flat output coupler (at 810–840 nm, $R_{out} = 70\%$). BRT is the three-plate birefringent tuner.

National Laboratory), placed around the Cr:LiSAF slab. The pump energy was focused on the sides of the Cr:LiSAF slab in a strip with dimensions of ~8.9 mm (length) and ~1.61 mm (height). The pump beam polarization was parallel to the *c*-axis of the crystal. The pump pulse duration and pulse repetition rate were 74 μs and 1 Hz, respectively. The laser cavity consisted of a HR concave mirror ($r_c = 200$ cm), two dielectric flat HR mirrors (45° for π-polarization), and an output coupler ($R_{out} = 70\%$). The single TEM_{00} transverse mode operation, with a mode diameter of ~1.5 mm inside the Cr:LiSAF crystal, was achieved with the cavity length of 1.2 m. The laser beam was diffraction limited ($M^2 \sim 1$) for all used power levels. The external TIR incident angle of 11.3° was chosen to produce a good overlap between the TEM_{00} transverse cavity mode and the pumped area of the crystal. For wavelength tuning and narrowing of the laser output line width, a three-plate BRT tuner was utilized, similar to the one described for the previous laser. A 1 m focal length, 0.1 nm resolution Czery-Turner spectrometer with diode array readout was used to monitor the wavelengths of the Cr:LiSAF lasers.

3. Experimental results

Before we present the experimental data about Cr:LiSAF laser output line width, let us consider the theoretically expected value of the laser line width assuming a homogeneously broadened emission line for the $^4T_2$-$^4A_2$ transition of Cr^{3+}-ions in the crystal. It is well known that, in free running operation, the laser line width (without any special wavelength selection in the cavity) depends on two factors: (1) the nature of the spectral broadening of the emission line of the active medium, and (2) intracavity spatially inhomogeneous distribution of the cavity mode fields, which leads to a multi-mode regime due to the 'spatial hole burning' effect [11]. Suppose that the laser emission line is homogeneously broadened and the active medium fills all the cavity space between mirrors. It is also assumed that the laser operates only on TEM_{00} transverse mode, and all of the longitudinal modes have equal losses. In this case, the laser output spectral half-width (FWHM), $\Delta\nu_{out}$, due to longitudinal mode 'spatial hole burning' in the standing wave resonator is calculated by using [12,13]

$$\Delta\nu_{out} = \left(\Delta\nu_{mod}\Delta\nu_{line}^2\frac{p-1}{p}\right)^{1/3} \qquad (1)$$

where $\Delta\nu_{mod} = c/2L$ is the laser resonator longitudinal mode spacing, c is a speed of light, L is the laser cavity length, $\Delta\nu_{line}$ is the laser active medium emission line width (FWHM), and p is the pump power measured relative to the laser threshold pump power.

The emission line width, $\Delta\nu_{line}$, of the $^4T_2$-$^4A_2$ laser transition of Cr^{3+}-ions in $LiSrAlF_6$ crystal is quite broad, with a full width at half maximum of about 200 nm ($\Delta\nu_{line} = 8.8 \times 10^{13}$ Hz) [1]. Fig. 3 (curves 3 and 4) shows a Cr:LiSAF laser line width, $\Delta\nu_{out}$, calculated from (1), which is theoretically expected for a homogeneously broadened emission line, depending on relative pump power p for a laser cavity length of $L = 20$ cm (this corresponds to an end-pumped Cr:LiSAF laser), and for a cavity length of $L = 120$ cm (this corresponds to TIR cavity laser). One can see, that, for a moderate value of the relative laser pump power, $p \sim 2$ to 2.5, calculated value of the first laser line width due to a 'spatial hole burning' effect would not exceed of ~3.4 nm, and the maximum expected value of the laser line width for an extremely high pumping ($p > 100$) would be only ~4.0 nm. For the second laser, the calculated line width is ~1.7–1.8 nm for $p \sim 2 \div 2.5$, and ~2.2 nm for $p > 100$, accordingly.

In Fig. 3, experimental values of the Cr:LiSAF laser line width versus the relative laser pump power, p, are also shown, both for end-pumped, and for TIR cavity laser (curves 1 and 2). It is seen that for both the investigated lasers, experimental values of laser line width are always much larger than linewidths calculated with the assumption

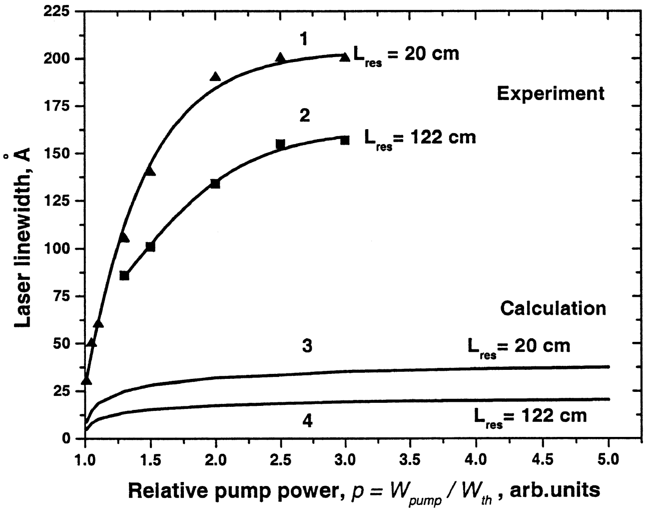

Fig. 3. Laser line width depends on the relative pump power. 1, 2—experimental data; 3, 4—calculation, according to Eq. (1). Curves 1 and 3 correspond to the end-pump laser with cavity length of $L_{res} = 20$ cm; curves 2 and 4 correspond to the TIR cavity laser with resonator length of 122 cm.

of homogeneously broadened laser emission line, where only a 'spatial hole burning' effect is taking into account. For example, the measured output line width of the end-pumped Cr:LiSAF laser was found to spread to 14 nm for the relative pump power of $p = 1.5$, while expected value of line width, calculated from (1), is only 3.0 nm. The similar ratio between experimental and calculated values of laser line width is observed for a TIR Cr:LiSAF laser: 13 and 2 nm, correspondingly.

This large difference between experimentally observed and calculated values of the laser line width clearly indicates the existence of another mechanism for the laser line width broadening than a 'spatial hole burning' effect in Cr:LiSAF lasers. The most likely, reason is some inhomogeneous to the broadening of the Cr:LiSAF crystal emission line of the $^4T_2$-$^4A_2$ transition of Cr^{3+}-ions. In addition with the broadening of laser output line width, inhomogeneous broadening should lead to a reduction of the laser output power, when the laser line width is made very narrow. In other words, the reduction in output power of a single longitudinal mode laser will be a function of the relative inhomogeneity of its emission line, where we define relative inhomogeneity as the ratio between the inhomogeneous and homogeneous width of the emission line. This dependence can be used for the quantitative estimation of inhomogeneous broadening of the Cr:LiSAF laser emission line. To do this, we need to calculate the output power of a single mode laser with inhomogeneously broadened emission line.

4. Analysis of inhomogeneous broadening

Inhomogeneous broadening can be considered as being the result of homogeneous broadened emissions from several groups of excited ions each of which emits at slightly different central frequency ν_0 as shown schematically in Fig. 4. Here we present a simple analysis to estimate the extent of the inhomogeneous broadening of Cr:LiSAF emission line by making some simplifying assumptions. Suppose that the upper and lower levels of a laser transition have only one Stark component, the lower laser level is always empty (four-level laser scheme), and laser runs at a single longitudinal mode with uniform transverse mode intensity distribution (the TEM_{00} transverse mode distribution is also adequate to this approach). The rate equations for the spectral density of the laser population inversion $N(\nu, t)$ and the intra-cavity single laser mode energy density $U_0(t)$ for an inhomogeneously broadened laser emission line is given by [6,14]

$$\frac{\partial N(\nu,t)}{\partial t} = W_p G(\nu,\nu_0) - \frac{N(\nu,t)}{\tau_{21}} = B_{21} N(\nu,t) g(\nu,\nu_0) U_0(t) \frac{N(\nu,t) - N^0 G(\nu,\nu_0)}{\tau_m} \quad \text{(2a)}$$

$$\frac{\partial U_0(t)}{\partial t} = B_{21} h\nu_0 U_0(t) \int_0^\infty g(\nu,\nu_0) N(\nu,t) d\nu - \gamma U_0(t) \quad \text{(2b)}$$

where W_p is a pump rate, equal to the number of ions excited per second in a unit volume. $G(\nu, \nu_0)$ is the function that describes an inhomogeneous broadened wavelength distribution of the various types of emitting ions in the active medium, centered at frequency ν_0. ν is the current frequency, and $g(\nu, \nu_0)$ is a function that describes a homogeneously broadened wavelength distribution of only one

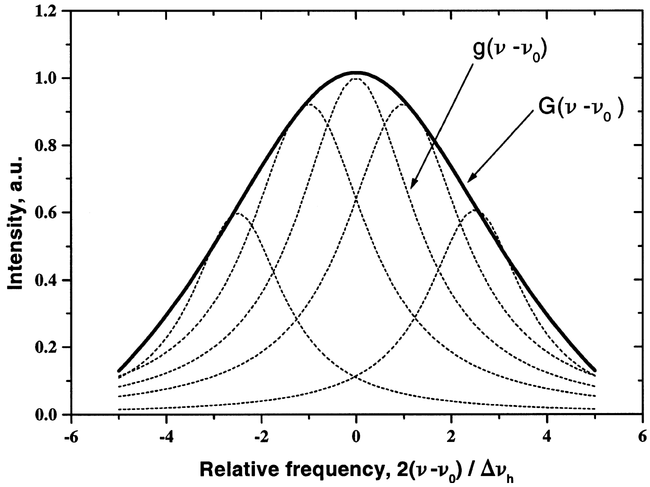

Fig. 4. Entire structure of the inhomogeneously broadened laser emission line used in our calculations. $g(\nu, \nu_0)$ is a function of a homogeneously broadened wavelength distribution of only one type of emitting ions, centered at frequency of ν_0; $G(\nu, \nu_0)$ is the function of an inhomogeneous broadened wavelength distribution of the various types of emitting ions in the active medium, centered at frequency ν_0.

type of emitting ions, centered at frequency of ν_0.τ_{21} is the upper laser level lifetime, and B_{21} is the Einstein coefficient for the laser transition at frequency ν_0. γ is the laser cavity losses, and $h\nu_0$ is the laser photon energy. τ_m is the migration time of the excited energy between different neighboring ions in the active medium, and $N^0 = \int_\nu N(\nu, 0)\mathrm{d}\nu$ is the initial density of the excited ions in active medium.

Assuming the line shape of $g(\nu, \nu_0)$ is represented by Lorenz profile

$$g(\nu, \nu_0) = \frac{2}{\pi\Delta\nu_h}\frac{1}{1+\dfrac{4(\nu-\nu_0)^2}{\Delta\nu_h^2}} \tag{3}$$

where $\Delta\nu_h$ is the half-width of the homogeneous broadened line $g(\nu, \nu_0)$.

The inhomogeneous distribution of $G(\nu, \nu_0)$ can be represented by Gaussian profile

$$G(\nu, \nu_0) = \frac{2}{\Delta\nu_{inh}}\frac{(\ln 2)^{1/2}}{\pi^{1/2}}\exp\left(-\frac{4\ln 2(\nu-\nu_0)^2}{\Delta\nu_{inh}^2}\right) \tag{4}$$

where $\Delta\nu_{inh}$ is the half-width of the inhomogeneously broadened line $G(\nu, \nu_0)$. Thus, the whole laser emission line shape is represented by the Voigt profile.

For the Cr:LiSAF crystal, we can also assume that the speed of migration τ_m^{-1} is equal to zero, because experimental data show a negligible value of emission quenching even for high doped Cr:LiSAF crystals [8]. For cw and quasi-cw pulsed regime, Eq. (2a and b) can be simplified, because

$$\frac{\partial N(\nu, t)}{\partial t} = \frac{\partial U_0}{\partial t} = 0 \tag{5}$$

and this set of equations can be solved for the Voigt shape of the laser emission line.

To compare the output of single longitudinal mode lasers with inhomogeneously and homogeneously broadened lines in identical conditions, (i.e. with the same relative pump power, p), we need to define and compare threshold pump powers for both.

Assuming the laser mode intensity is given by $U_{0,inh} = 0$, and taking into account Eq. (5), we can derive from Eq. (2a and b) the threshold pump power, $W_{th,inh}$, of a laser with an inhomogeneously broadened emission line as

$$W_{th,inh} = \frac{\gamma}{B_{21}\tau_{21}h\nu_0\int_0^\infty g(\nu, \nu_0)G(\nu, \nu_0)\mathrm{d}\nu} \tag{6}$$

Accordingly, the threshold pump power, $W_{th,h}$, of a laser with a homogeneously broadened line can be represented as

$$W_{th,inh} = \frac{\gamma}{B_{21}\tau_{21}h\nu_0\int_0^\infty g_h(\nu, \nu_0)\mathrm{d}\nu} \tag{7}$$

where $g_h(\nu, \nu_0)$ is Lorenz profile of the homogeneous broadened emission line with a half-width of $\Delta\nu_{line,h}$.

Comparison of Eqs. (6) and (7) shows that the threshold pump powers of these two lasers are equal on the condition of equal spectral widths of their emission lines. This corresponds to

$$\int_0^\infty g(\nu, \nu_0)G(\nu, \nu_0)\mathrm{d}\nu = \int_0^\infty g_h(\nu, \nu_0)\mathrm{d}\nu \tag{8}$$

Substitution of Eqs. (3) and (4) into Eq. (8) determines the half-width of an inhomogeneously broadened laser emission line with the Voigt profile, $\Delta\nu_{line,inh}$, defined by means of $\Delta\nu_{inh}$ and $\Delta\nu_h$, that corresponds to the same threshold pump power as a homogeneously broadened emission line would have with an equal half-width

$$\Delta\nu_{line,inh} = \Delta\nu_h\frac{\sqrt{\pi}}{aQ(\beta)} = \Delta\nu_{line,h} \tag{9}$$

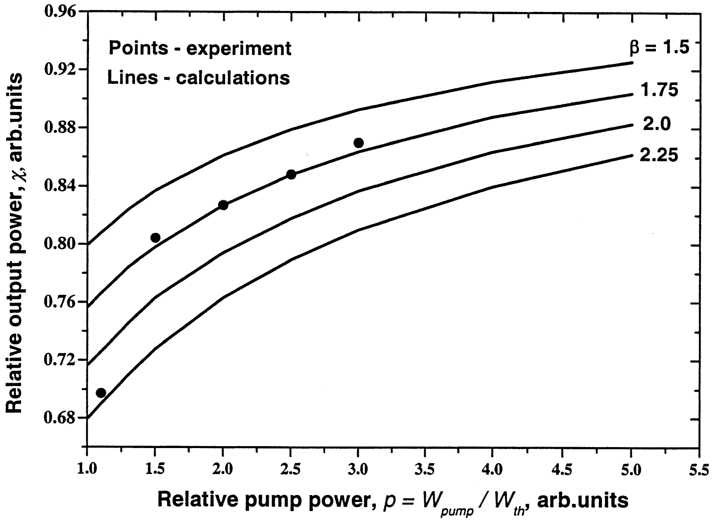

Fig. 5. Relative reduction in laser output which is caused by inhomogeneously broadened laser emission line. $\beta = \frac{\Delta \nu inh}{\Delta \nu h}$ is a parameter of inhomogeneity of the emission line. Lines correspond to calculations by Eq. (18) with different value of β. Points are experimental data, received with the second laser.

where

$$a = \frac{\sqrt{\ln 2}}{\beta} \quad (10)$$

$$\beta = \frac{\Delta \nu_{\mathrm{inh}}}{\Delta \nu_{\mathrm{h}}} \quad (11)$$

is a parameter of inhomogeneity of the emission line;

$$Q(\beta) = 2\int_0^\infty \frac{\exp(-2a^2x^2)}{1+x}\,\mathrm{d}x \quad (12)$$

and

$$x = \frac{2(\nu - \nu_0)}{\Delta \nu_{\mathrm{h}}} \quad (13)$$

is a relative frequency.

It should be noted that $\lim_{\beta \to 0}\{a(\beta)Q(\beta)\} = \sqrt{\pi}$, and Eq. (9) goes to correct limit with $\beta = 0$ (i.e. the case of no inhomogeneity).

Solving Eq. (2a and b) for the case of $U_0 \neq 0$ and the Voigt emission line profile, we have the equation for the laser mode intensity A_{inh}

$$\int_0^\infty \frac{\exp(-a^2x^2)}{1 + A_{\mathrm{inh}} + x^2}\,\mathrm{d}x = \frac{Q(\beta)}{2p} \quad (14)$$

where $Q(\beta)$ and a are given by Eqs. (12) and (11);

$$A_{\mathrm{inh}} = \frac{B_{21}h\nu_0\tau_{21}2U_{0,\mathrm{inh}}}{\pi \Delta \nu_{\mathrm{inh}}} \quad (15)$$

is normalized mode intensity of the laser with inhomogeneously broadened emission line, and $p = W_{\mathrm{p}}/W_{\mathrm{th}}$ is the relative pump power.

Eq. (14) can be solved numerically to find the dependence of $A_{\mathrm{inh}} = f(\acute{u}, p)$.

The normalized mode intensity of the laser with the homogeneously broadened emission line (Lorenz profile), A_{h}, as a function of the relative pump power can be easily derived from Eq. (2a and b)

$$A_{\mathrm{h}} = p - 1 \quad (16)$$

where

$$A_{\mathrm{h}} = \frac{2B_{21}h\nu_0\pi_{21}U_{0,\mathrm{h}}}{\pi \Delta \nu_{\mathrm{line,h}}} \quad (17)$$

The ratio between $U_{0,\mathrm{inh}}$ and $U_{0,\mathrm{h}}$ gives the relative reduction of the laser output in a single longitudinal mode regime which is caused by inhomogeneous broadening of the laser emission line. By using Eqs. (14) and (16), and taking into account Eqs. (9), (15) and (17), we can find this ratio (it should be noticed that this output reduction will be negligibly small for the multi-mode regime).

$$\chi(\beta, p) = \frac{U_{0,\mathrm{inh}}}{U_{0,\mathrm{h}}} = \frac{A_{\mathrm{inh}}2aQ(\beta)}{(p-1)\pi^{1/2}} \quad (18)$$

Because this ratio is a function of the parameter of inhomogeneity of the emission line, β, we can compare experimental data and calculated from Eq. (18) for various values of parameter β in order to do the estimation of the inhomogeneous broadening of the Cr:LiSAF emission line. Fig. 5 shows curves calculated from Eq. (18) giving χ as a function of p for $\beta = 1.5$, 1.75, 2.0 and 2.25. Experimental data received with TIR cavity laser, (i.e. the ratio of the Cr:LiSAF laser output energy in the narrow-line width and in multimode regime), are represented by points on the same plot. The best fit between the calculated and experimental data is observed for a parameter of inhomogeneous broadening of the Cr:LiSAF emission line of $\beta \sim 1.75$. This inhomogeneous broadening parameter is fairly small, when compared, for example, with neodymium glasses that have β values of $\beta \approx 4$–6. Nevertheless, inhomogeneous broadening can be responsible for an unexpectedly wide Cr:LiSAF laser line width, and also for the reduction in the laser output. Thus for narrow line width operation we can expect the reduction in the Cr:LiSAF laser output of approximately 15–20% compared with wide bandwidth operation for the values of the relative pump power $p \sim 2$–3.

5. Conclusion

In free running operation, Cr:LiSAF lasers exhibit a large line width that cannot be explained only by 'spatial hole burning' effects in a standing-wave resonator. By including the possibility of a slight inhomogeneous broadening of the Cr:LiSAF emission line, corresponding to the $^4T_2$-$^4A_2$ transition of Cr^{3+}-ions, the observed laser line width can be explained. The relative reduction of the laser output in a single longitudinal mode regime which is caused by inhomogeneous broadening of the laser emission line has been calculated by means of a simple model. By comparing the measured laser output energy with the calculated laser output, the relative spectral inhomogeneity parameter of the Cr:LiSAF crystal emission line β is estimated to be $\beta = 1.6$–1.8.

References

[1] S.A. Payne, L.L. Chase, L.K. Smith, W.L. Kway, H.W. Newkirk, J. Appl. Phys. 66 (1989) 1051.
[2] S.A. Payne, L.K. Smith, R.J. Beach, B.H.T. Chai, J.H. Tassano, L.D. DeLoach, W.L. Kway, R.W. Solarz, W.F. Krupke, Appl. Opt. 33 (1994) 5526.
[3] M. Stadler, B.H.T. Chai, M. Bass, Appl. Phys. Lett. 58 (1991) 216.
[4] J.W. Early, C.S. Lester, C.R. Quick, J.J. Tiee, T. Shimada, N.J. Cockroft, OSA Proceedings on Advanced Solid-State Lasers, vol. 24, p. 9, B.H.T. Chai, S.A. Payne (Eds.), 1995.
[5] C.C. Johnson, D.J. Reichle, N.O. Barnes, G.J. Quarles, J.W. Early, N.J. Cockroft, Advanced Solid-State Lasers Vol 1 1996, p. 120.
[6] A.A. Mak, L.N. Soms, V.A. Fromzel, V.E. Yashin, 'Lasers na neodimovom stekle', Nauka, Moscow, 1990, p. 96.
[7] S.A. Payne, L.L. Chase, G.D. Wilke, J. of Luminescence 44 (1989) 167.
[8] S.A. Payne, W.F. Krupke, L.K. Smith, W.L. Kway, L.D. DeLoach, J.B. Tassano, IEEE J. of Quantum Electron. QE-28 (1992) 1188.
[9] C.R. Prasad, I.H. Hwang, V. Fromzel, Advanced Solid State Lasers, OSA Technical Digest, Optical Society of America, Washington DC, 1997, p. 42.
[10] V. Fromzel, C.R. Prasad, C. Johnson, N.P. Barnes, G.H. Kim, R.D. Mead, Conference on Lasers and Electro-Optics, OSA Technical Digest, Optical Society of America, Washington DC, 1999, p. 451.
[11] C.L. Tang, H. Statz, G.A. DeMars, J. Appl. Phys. 34 (1963) 2289.
[12] B.L. Livshizs, V.N. Zsikunov, Soviet J. of Experimental and Theoretical Phys. 49 (1965) 1843.
[13] Y.I. Hanin, Dinamika kvantovih generatorov, vol. 2, Sovetskoe Radio, Moscow, 1975, p. 215.
[14] A.J. Cabezas, R.P. Treat, J. Appl. Phys. 37 (1966) 3556.